Analyst

ROYAL SOCIETY OF CHEMISTRY

PAPER

View Article Online
View Journal | View Issue

Cite this: *Analyst*, 2025, **150**, 131

Real-time monitoring of vancomycin using a split-aptamer surface plasmon resonance biosensor†

Cátia Santa,[a] Soohyun Park,[a] Artur Gejt,[a,b] Heather A. Clark,[c] Bastian Hengerer[d] and Khulan Sergelen *[a]

Real-time monitoring of therapeutic drugs is crucial for treatment management and pharmacokinetic studies. We present the optimization and affinity tuning of split-aptamer sandwich assay for real-time monitoring of the narrow therapeutic window drug vancomycin, using surface plasmon resonance (SPR). To achieve reversible, label-free sensing of small molecules by SPR, we adapted a vancomycin binding aptamer in a sandwich assay format through the split-aptamer approach. By evaluating multiple split sites within the secondary structure of the original aptamer, we identified position 27 (P27) as optimal for preserving target affinity, ensuring reversibility, and maximizing sensitivity. The assay demonstrated robust performance under physiologically relevant ranges of pH and divalent cations, and the specific ternary complex formation of the aptamer split segments with the analyte was confirmed by circular dichroism spectroscopy. Subsequently, we engineered a series of split-aptamer pairs with increasing complementarity in the stem regions, improving both the affinity and limit of detection up to 10-fold, as compared to the primary P27 pair. The kinetics of the engineered split-aptamer pairs were evaluated, revealing fast association and dissociation rates, confirming improved affinity and detection limits across variants. Most importantly, the reversibility of the assay, essential for real-time monitoring, was maintained in all pairs. Finally, the assay was further validated in complex biological matrices, including the cerebrospinal fluid from dogs and diluted plasma from rats, demonstrating functionality in biological environments and stability exceeding 9 hours. Our study paves the way for applications of split-aptamers in real-time monitoring of small molecules, with potential implications for *in vivo* therapeutic drug monitoring and pharmacokinetic studies.

Received 17th September 2024,
Accepted 13th November 2024

DOI: 10.1039/d4an01226g

rsc.li/analyst

Introduction

The emergence of personalized medicine has increased the interest in real-time therapeutic drug monitoring (TDM). Currently, TDM relies on laboratory-based methods such as immunoassays or mass spectrometry, resulting in infrequent sampling and delayed results.[1] Furthermore, understanding the *in vivo* pharmacokinetic profile of a drug is essential to define its mechanism of action and bioavailability. These challenges underscore the need for point-of-care or *in vivo* strategies capable of real-time sensing. Various strategies of biosensing have been proposed to tackle real-time TDM,[2] yet, further refinement is needed to ultimately enhance therapeutic interventions, reduce underdosing and toxicity-related effects, and potentially accelerate drug discovery and development processes.[3]

Vancomycin, a 1450 Da hydrophilic glycopeptide and broad spectrum antibiotic, plays a critical role in managing methicillin-resistant *Staphylococcus aureus* (MRSA) and central nervous system (CNS) infections.[4,5] The narrow therapeutic window and high interpatient variability necessitate accurate, personalized dosing regimens.[5] While there is an increasing demand for improved TDM and pharmacokinetic (PK) studies of vancomycin in blood,[6] the need is particularly acute for CNS conditions, as a first-line antibiotic treatment for intracranial

[a]*BioMed X Institute, Heidelberg, Germany. E-mail: sergelen@bio.mx*
[b]*Faculty of Biotechnology, Mannheim University of Applied Sciences, Germany*
[c]*School of Biological and Health Systems Engineering, Arizona State University, USA*
[d]*Boehringer Ingelheim Pharma GmbH & Co. KG, CNS Research, Germany*

† Electronic supplementary information (ESI) available: Full sensorgram of the P27 pair challenged with different vancomycin concentrations; the CD spectrum of the P27 pair with and without vancomycin and the negative control sequence; the sensorgram and dose–response curves for full-aptamer measurements under flow; complete sensorgrams of cycles 1 and 2 for the 5 tested aptamer pairs; the predicted structure and dose–response curve for the P27.2.02 pair; the SDS-PAGE protein profile of diluted plasma and dog CSF. A table describing the sequences of all the oligonucleotide molecules used. See DOI: **https://doi.org/10.1039/d4an01226g**

infection after surgery.[4] Limited knowledge of the dynamics of vancomycin in the CNS, coupled with reliance on blood-based estimations, may lead to suboptimal dosing.[4,7]

Among various real-time sensing techniques, surface plasmon resonance (SPR) is a gold-standard technology widely used for analytical purposes and kinetics analysis of binding events. SPR provides mass-dependent, real-time optical signals upon target analyte binding to a specific immobilized receptor and allows for robust, label-free and real-time molecular monitoring.[8] To achieve these criteria, bioreceptors with affinities weaker than the typical pM–nM ranges and rapid dissociation rates are needed to allow reversible sensing.[9,10] Aptamers are particularly well-suited for establishing reversible biosensors due to their ease of modification and adaptability.[11–14] Molecular detection using SPR biosensors is dependent on the refractive index change caused by bound molecules within tens of nanometers from the gold surface and therefore does not require the aptamer conformational change within a few nanometers of the sensor surface necessary for electrochemical[6,15] or transistor-based sensors.[16–18]

In this report, we present a robust approach to monitor small molecules using SPR through a sandwich assay based on the aptamer splitting strategy that enhances the SPR signal by creating a three-component complex upon vancomycin binding. This results in a substantially increased change in the local refractive index compared to single-aptamer direct sensing. The amplification effect is of particular interest for detecting small molecules, like vancomycin, which typically generate weak SPR signals due to their low molecular weight. The dynamic nature of the split-aptamer–vancomycin interaction allows for real-time monitoring and sensor regeneration without the need for additional labeling,[19] enhancement steps[20] or complex regeneration protocols,[21] which are difficult strategies to implement for *in vivo* measurements. In this study, we have identified a functional splitting site, characterized the resulting assay performance, explored affinity-enhancing modifications, and confirmed the structural integrity *via* circular dichroism (CD) spectroscopy. We tested our sensor under physiologically relevant conditions and matrices to evaluate the feasibility for potential *in vivo* monitoring applications. To our knowledge, this represents the first application of a split-aptamer sandwich assay for monitoring vancomycin on SPR and forms the basis for studying split-aptamer tunability and adaptability for reversible monitoring of small molecules with the specific aim for potential applications in therapeutic drug monitoring and pharmacokinetic studies.

Experimental section

Chemicals and materials

All DNA oligonucleotide sequences were ordered from Integrated DNA Technologies (sequences described in ESI Table 1†). Vancomycin hydrochloride, rat plasma, MES (2-morpholinoethanesulfonic acid) monohydrate and ethanolamine were acquired from Sigma-Aldrich. UltraPure™ distilled water, 10× concentrated phosphate-buffered saline (PBS) pH 7.4 (RNase-free), magnesium chloride, calcium chloride, sodium chloride, 1-ethyl-3-(3-dimethylaminopropyl)carbodiimide hydrochloride (EDC), *N*-hydroxysuccinimide (NHS), and neutravidin biotin-binding protein were purchased from Thermo Fisher Scientific. HPLC-grade ethanol was purchased from Carl Roth GmbH + Co. KG. Functionalized thiols (HS-(CH_2)m-EG_4-OH and HS-(CH_2)m-EG_6-OCH_2-COOH) were purchased from ProChimia Surfaces, and thiolated PEG (CH_3O-PEG-SH α-methoxy-ω-mercapto PEG) was purchased from Rapp Polymere GmbH. Dog cerebrospinal fluid (CSF) was kindly provided by Boehringer Ingelheim GmbH.

Sensor chip preparation

Bare gold coated prisms were acquired from Affinité Instruments, rinsed with 99% ethanol and dried under a stream of nitrogen. Prisms were incubated for at least 12 h in a 1 mM solution of carboxyl and hydroxyl thiols (1 : 9 ratio) after purging with nitrogen to form a self-assembled monolayer (SAM). Further functionalization of the chip and subsequent SPR measurements were performed in a P4SPR Quad Inlet Model system (Affinité Instruments). The sensor surface was passivated with 100 μM thiolated PEG for 30 min. Next, carboxyl moieties were activated through EDC and NHS, followed by 20 min incubation with neutravidin protein (50 μg mL^{-1} in MES buffer at pH 4.5) to covalently conjugate to the surface. Unreacted NHS ester groups were blocked by incubating with 1 M ethanolamine at pH 8, followed by immobilization of 1 μM 5′-biotinylated aptamer in PBS (pH 7.4) for 20 min. Lastly, 100 μM biotin in PBS was incubated for 10 min to block the remaining biotin-binding sites on neutravidin protein.

Steady-state SPR measurements

Vancomycin detection experiments in the steady state were performed using the P4SPR Quad Inlet Model (Affinité Instruments) at 37 °C. Samples with 2 μM free split-aptamer and increasing concentrations of vancomycin (0 μM to 100 μM or 250 μM) were injected and equilibrated for at least 5 min, followed by a washing step. All measurements were referenced to the same concentration of vancomycin without free aptamer. Aptamer–analyte complex measurements were performed in assay buffer (PBS with 2 mM $MgCl_2$ at pH 7.4) or artificial cerebrospinal fluid (aCSF)[22] (147 mM NaCl, 1.2 mM $MgCl_2$, 1 mM $CaCl_2$, 3.5 mM KCl, 2.5 mM $NaHCO_3$, 1 mM NaH_2PO_4). For testing ionic and pH influence, buffer concentrations of divalent cations and pH were modified. For complex matrix experiments, 200× diluted rat plasma in aCSF or dog CSF was used. The apparent dissociation constant (K_d) was calculated by fitting dose–response curves with the Hill equation and was determined as the half-maximum value. The limit of detection (LOD) was calculated as the intercept concentration with the mean of background signal plus 3 times the standard deviation (3σ) on a linear regression. Reversibility was quantified as the sensor response return to the baseline after reaching a plateau. It is expressed as the average percentage return to the baseline for sensor response at and above

the calculated LOD, across multiple concentrations. All data analyses were performed using Origin 2024 v10.1.

SPR measurements under flow

SPR measurements under flow were performed using a Biacore T200 with a similar setup to that of the steady-state measurements. A neutravidin-derivatized linear polycarboxylate hydrogel (30M, XanTec bioanalytics) sensor chip was conditioned with 40 mM NaOH and 1 M NaCl. Biotinylated aptamer sequences at 100 nM were immobilized on the surface by flowing for 240 s at a rate of 30 μL min^{-1}. Two measurement cycles were acquired for each aptamer pair. In cycle 1 (reference), 2 μM free aptamer was injected 5 times. Cycle 2 comprised 5 samples containing 2 μM free aptamer with different vancomycin concentrations (4-fold dilutions starting at 50 μM). Each cycle consisted of five injections of different concentrations, with 120 s contact time and 60 s dissociation per injection, followed by a final 300 s dissociation step. All measurements were performed at a flow rate of 30 μL min^{-1}. Dose–response curves were established by subtracting cycle 1 from cycle 2. Data analysis was performed similarly to the steady-state measurements.

Circular dichroism (CD) measurements

CD experiments were conducted using a Jasco J-715 spectrometer with a total volume of 150 μL in a 1 mm pathlength QS cuvette. Scans were performed from 200 to 320 nm at 37 °C in continuous scan mode at a speed of 200 nm min^{-1}, with a response time of 1 s and a 0.2 nm bandwidth. Each measurement was an average of 5 scans. All experiments were performed in assay buffer (PBS with 2 mM $MgCl_2$), using 10 μM split-aptamer and 100 μM vancomycin. Due to the strong CD absorbance, the spectrum from vancomycin was subtracted from the vancomycin–aptamer complex spectrum.

Results and discussion

We present the split-aptamer sandwich assay strategy for real-time, reversible detection of vancomycin using SPR under physiologically relevant conditions of the brain tissue. Our approach adapts an aptamer sequence originally developed for an *in vivo* electrochemical sensor,[12] optimizing it for SPR-based label-free detection. By strategically splitting the original aptamer into two segments, we aimed to engineer bioreceptor (s) with enhanced sensitivity and specificity for real-time detection of low molecular-weight molecules (Fig. 1A). The split-aptamer strategy enhances the SPR signal by leveraging two segments of the original aptamer: one immobilized on the SPR surface (split 1) and the other free-floating in solution (split 2) (Fig. 1B). Although further enhancement of the SPR signal for split-aptamer assays through the use of fluorophores[9] and gold nanoparticles[20,23] is reported, we have opted to simplify the characterization of binding interactions by label-free detection. In the presence of vancomycin, both segments that otherwise have low complementarity bind to the target molecule, forming a three-component complex. This complex generation results in a two-fold amplification of the

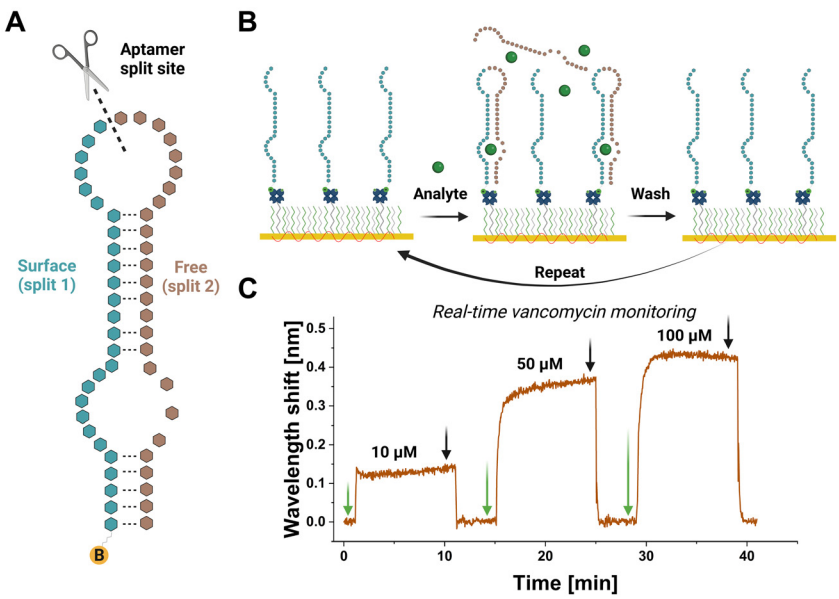

Fig. 1 Schematic depiction of the split-aptamer-based reversible assay for vancomycin detection on SPR. (A) Illustration of the aptamer split site position within the full aptamer. The biotinylated segment (split 1) is immobilized on the sensor chip surface, while the free segment (split 2) remains in solution. (B) SPR sensor surface architecture, highlighting key components and experimental steps: (1) immobilized split 1, (2) split 2 in solution together with vancomycin forming the split-aptamer–vancomycin complex, and (3) washing of split 2 and vancomycin for sensor reversibility. (C) Representative sensorgram demonstrating reversible vancomycin detection. The graph shows the SPR response to increasing concentrations (10, 50, and 100 μM) of vancomycin (green arrows), followed by buffer wash steps (black arrows) to demonstrate the sensor reversibility.

SPR signal compared to traditional single-aptamer methods, permitting the detection of small molecules like vancomycin.[8] Furthermore, our system enables real-time and reversible detection of vancomycin concentrations, as demonstrated by the representative sensorgram (Fig. 1C). The reversible nature of the aptamer–vancomycin interaction allows for continuous measurements and sensor recovery through buffer washes, highlighting the potential for real-time monitoring applications.

Split-aptamer sandwich assay development

To develop the sandwich assay for vancomycin detection using split-aptamer pairs, we evaluated three potential splitting sites within the aptamer sequence: positions 16 (P16) and 18 (P18) within the predicted internal stem and position 27 (P27) in the upper loop (Fig. 2A). The first biotinylated aptamer segment (split 1) was tethered to the sensor surface, while the other segment (split 2) remained freely floating in solution with or without the analyte. We chose two split sites within the stem structure, P16 and P18, respectively to test the effect on the integrity of the vancomycin-binding pocket, hypothesizing it to be in the lower loop region. Introducing split sites progressively moving further from the lower loop region was expected to improve the signal-to-noise ratio by having a greater contrast between bound and unbound states, unless the binding site was directly disrupted. Position P27 was selected to preserve the stem structure while potentially allowing for conformational changes upon vancomycin binding. At physiological temperature, we predict[24] that the aptamer secondary structure in the absence of analyte will have low stability and therefore permit enhanced contrast between free and ternary complexed states.

Split sites P16 and P18 resulted in non-functional aptamer pairs at tested vancomycin concentrations between 5 and 250 μM (Fig. 2B). The loss of functionality may be attributed to hindered secondary structure formation of the aptamer, potentially disrupting vancomycin binding. Interestingly, P18 shows very weak binding in contrast to P16, and this leads us to presume the binding site is closer to the lower part of the stem region. On the other hand, P27 demonstrated binding functionality, exhibiting a dose-dependent response to increasing vancomycin concentrations. These results indicate that the

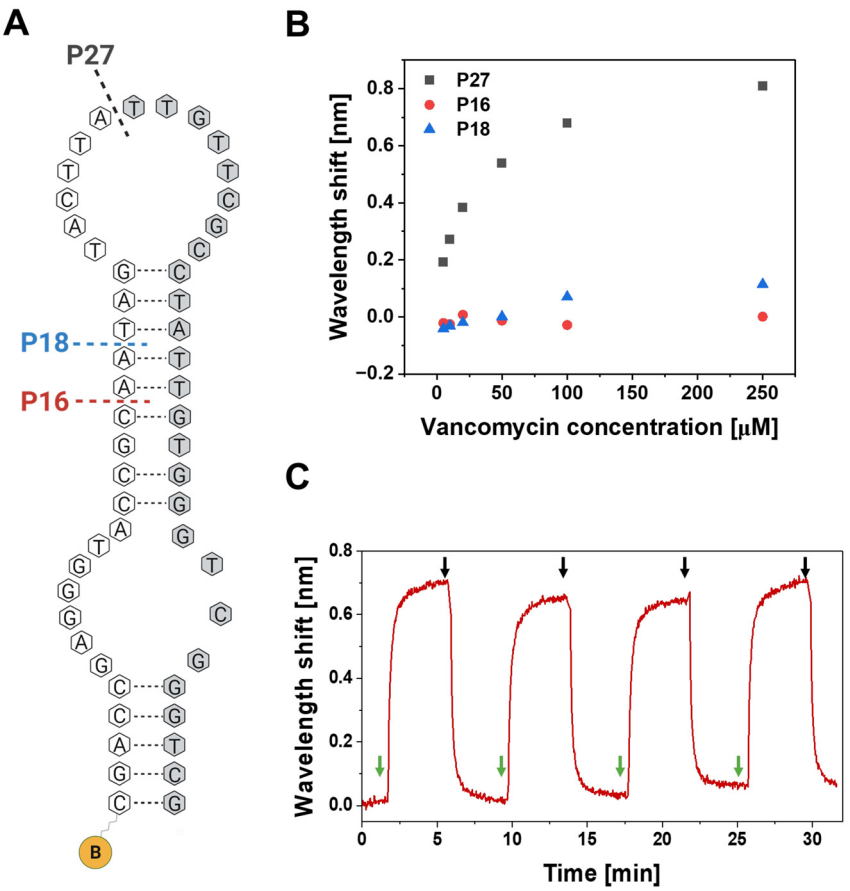

Fig. 2 Characterization of full-length and split-aptamer variants for vancomycin detection. (A) Schematic representation of the aptamer sequence, indicating the investigated split positions (P16, P18, and P27). The biotinylated segment (yellow) is tethered to the sensor surface, while the other segment remains free in solution. (B) Dose–response curves for three split-aptamer pairs. (C) Repeatability and reproducibility assessment of the P27 split-aptamer pair. The sensorgram shows four consecutive measurements of 50 μM vancomycin. Green arrows indicate vancomycin injection; black arrows represent buffer wash steps.

internal stem region integrity could be crucial for vancomycin binding for this aptamer. The upper loop can be seen as a flexible region not contributing strongly to vancomycin binding. Our findings are in agreement with the reported *in silico* determination of the binding sites[14] of the aptamer to vancomycin. Henceforth, we applied the P27 split-aptamer pair for further optimization and characterization of our assay.

As reversibility and reproducibility are essential requirements for real-time molecular monitoring, we subsequently characterized these fundamental properties of our P27 split-aptamer pair. The sensorgrams obtained for each injection cycle reveal that the formation of the aptamer–vancomycin complex is fully reversible upon depletion of the analyte from the system, with fast association and dissociation rates occurring within seconds (Fig. 2C). This full reversibility contributes to a high level of reproducibility, as evidenced by consistent responses to repeated exposures of a constant vancomycin concentration. Moreover, when testing the assay with alternating and gradual increasing and decreasing concentrations of vancomycin (ESI Fig. 1†), we observed consistent responses to identical concentrations and a constant return close to the baseline upon washing, further validating the suitability of our system for real-time molecular monitoring.

To further validate the formation of the aptamer–analyte–aptamer complex, we conducted circular dichroism (CD) spectroscopy studies in the presence and absence of vancomycin (ESI Fig. 2†). The observed peak shift in the 250–280 nm range is comparable to that reported for the full-length aptamer,[6] providing additional evidence for the specific binding interaction. Importantly, when one part of the split-aptamer was replaced with a random DNA sequence (negative control, NC), no peak shift was observed, confirming that the complex formation is sequence-specific to our designed split-aptamer. These spectroscopic results corroborate our SPR findings and further support the efficacy of our split-aptamer approach in capturing and detecting vancomycin through the formation of a specific ternary complex.

Split-aptamer assay under physiologically relevant conditions

To assess the potential for deploying our assay in complex, physiologically relevant samples, we evaluated its performance under conditions mimicking the natural variations in living brain tissue of rodents. We compared dose-dependent responses in our standard assay buffer to those in artificial cerebrospinal fluid (aCSF), a physiologically relevant buffer (Fig. 3A). We observed that the limit of detection (LOD) remained comparable at 6.9 μM in aCSF *versus* 9.9 μM in assay buffer. This demonstrates the robustness of our split-aptamer assay under different buffer conditions.

We further evaluated the assay performance across physiologically relevant ranges of pH and divalent cation concentrations typical in rodent brain models. The pH fluctuations in the brain extracellular space are known to have modulatory effects, with relevant pH levels of 6.5 to 8[27] and an average of 7.3 measured in the CSF.[28] The responsiveness of the aptamer pair was tested to a fixed concentration of vancomycin in PBS buffer with 2 mM $MgCl_2$ across the relevant pH range (Fig. 3B). Our results show that the assay response remains largely consistent across most tested pH levels, with no significant response difference. However, at pH 6.5, we noted an approximately 20% increase in response. This pH represents the lower limit of what can be expected *in vivo* and would be indicative of moderate acidosis, potentially caused by conditions such as ischemia.[29] Nonetheless, our pH stability profile demonstrates the robustness of our split-aptamer assay across a range of physiologically relevant conditions, and it warrants consideration, particularly for future studies in disease states where pH fluctuations can be more pronounced.

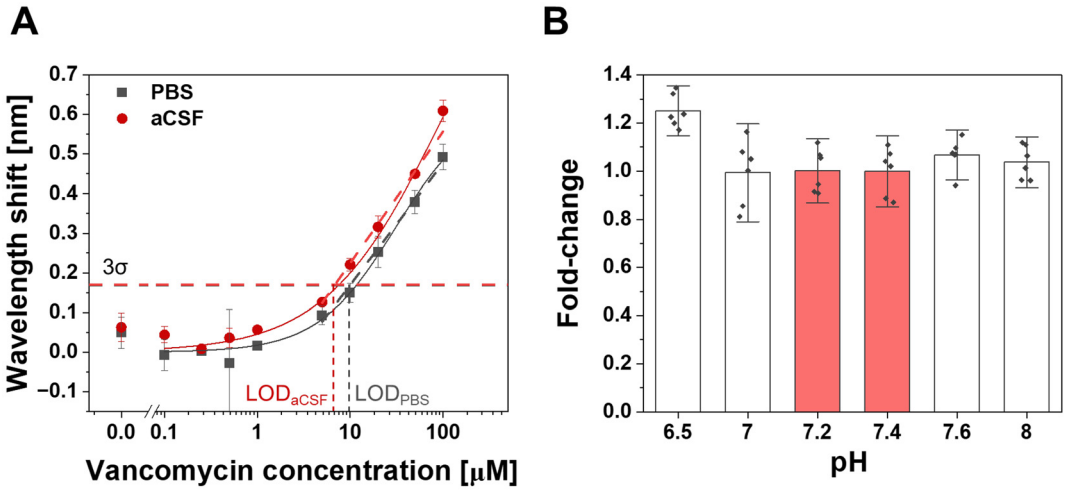

Fig. 3 Characterization of P27 split-aptamer assay robustness under varying physiological conditions. (A) Dose–response curves of the P27 split-aptamer pair in standard assay buffer and aCSF. (B) Normalized response of the aptamer pair to 100 μM vancomycin in assay buffer (PBS with 2 mM $MgCl_2$) at different pH values. Values are normalized to the response at pH 7.4. Highlighted areas represent the physiologically reported ranges.[25,26] Error bars represent the standard deviation.

We further investigated the influence of divalent cations on our split-aptamer assay as these ions can significantly affect aptamer molecular interactions and structural configurations.[22] This validation is particularly relevant for potential *in vivo* deployments, where physiological fluctuations of these cations occur naturally during neuronal activity. In the brain, physiological concentrations range between 0.8 and 1.2 mM for magnesium[25] and approximately 1 mM for extracellular calcium,[26] with 1.2 mM reported in the CSF[30] (ESI Fig. 3†). Our results demonstrate that variations in magnesium and calcium concentrations within physiologically relevant ranges do not significantly influence the assay response to vancomycin. This robustness to divalent cation fluctuations is crucial, as it suggests that the sensor performance should remain consistent across the range of ionic conditions typically encountered in the brain microenvironment. Overall, the stability of our assay across these varying pH and ionic conditions further supports its potential for reliable *in vivo* vancomycin monitoring, where local fluctuations in pH and ion concentrations are expected and should not interfere with the signal output.

Affinity tuning of split-aptamer for increased sensor sensitivity

The clinically relevant concentration range of vancomycin in blood typically falls between 6 and 30 μM.[6,31] In mouse cortex studies using an aptamer-based electrochemistry sensor, a peak vancomycin concentration of ~8 μM was observed following an I.V. bolus of 75 mg kg^{-1},[6] and in the lateral ventricle, following 40 mg kg^{-1} I.V., the peak concentration was registered at 14 μM.[32] Our initial split-aptamer P27 assay demonstrated a limit of detection (LOD) of 9.9 μM in assay buffer, which, while close, falls short of the required sensitivity for these lower physiological concentrations. To enhance the sensitivity of our assay while retaining reversible interactions, we systematically explored several modifications to the split-aptamer sequence (Fig. 4A). Our goal was to fine-tune the affinity within a range that would improve the detection of

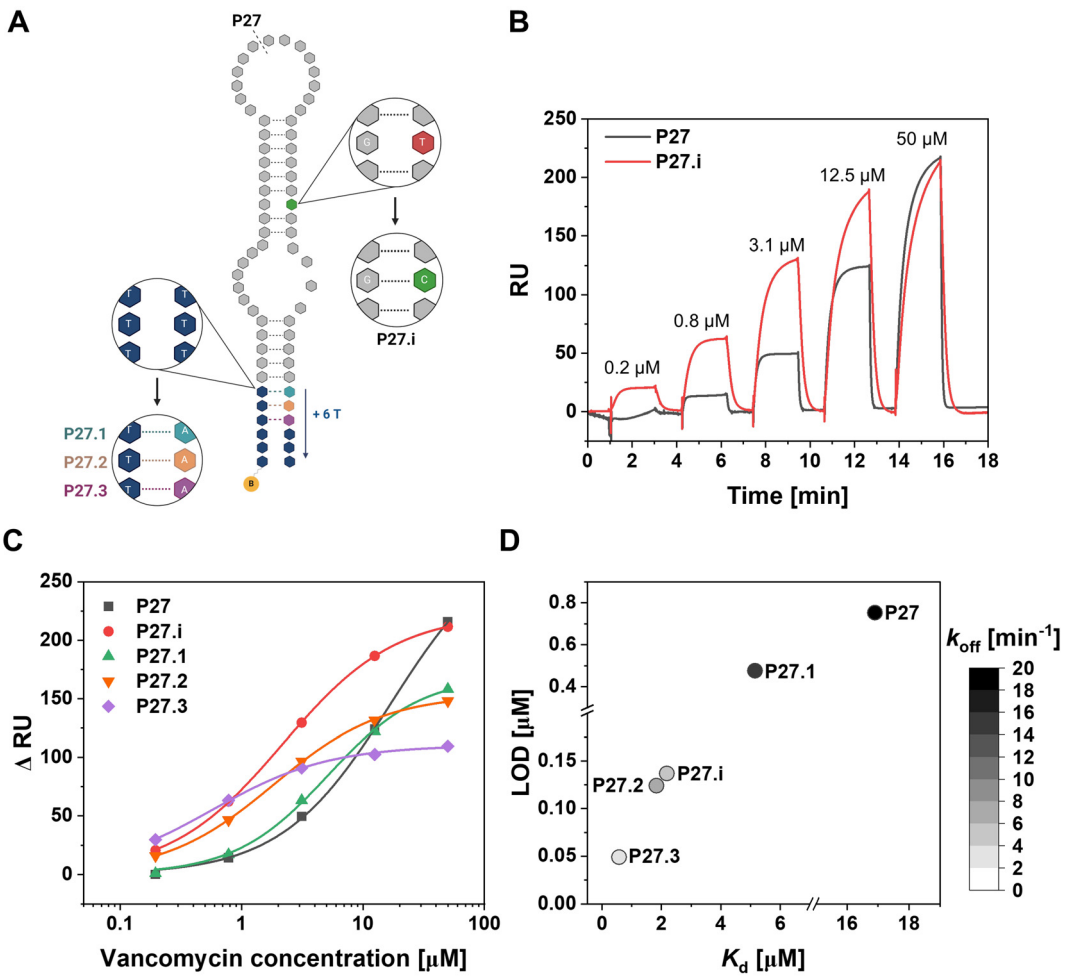

Fig. 4 Evaluation of modified split-aptamer pairs under flow conditions. (A) Schematic representation of sequence modifications in the internal stem (P27.i) and lower stem extensions (P27.1, P27.2, and P27.3) of the original split-aptamer pair, P27. (B) Full sensorgrams of P27 and P27.i. (C) Dose–response curves demonstrating affinity tuning by increasing hybridization in the stem region. (D) Summary matrix presenting K_d, LOD, and k_{off} values for each tested aptamer pair, illustrating the impact of structural modifications on binding kinetics and assay sensitivity.

clinically relevant vancomycin concentrations without compromising the reversibility of the sensor. We tested several structural modifications, focusing on alterations in the internal stem region and extensions of the lower stem. To characterize the performance and kinetics of our split-aptamer system, we conducted measurements under flow conditions using the highly sensitive Biacore SPR device, contrasting with the steady-state conditions described in previous sections.

Firstly, we evaluated the full-length original aptamer for direct vancomycin detection. The resulting specific dose–response curve yielded a K_d of 250 nM (ESI Fig. 4),† which aligns well with the previously reported K_d of 140 nM.[6,12] However, the response window for this full-length aptamer assay was notably small (~30 RU in total), highlighting the challenges of direct vancomycin detection for potential *in vivo* measurements using SPR. Our split-aptamer approach addresses this limitation by significantly amplifying the SPR signal (~10-fold), as demonstrated by the improved sensitivity and broader response ranges observed in our modified split-aptamer variants.

We designed four different P27 derivatives to increase the base-pair interactions, hypothesizing that enhanced stability of the aptamer–analyte–aptamer complex would improve affinity and sensitivity. Our initial modification addressed a single base-pair mismatch in the internal stem of the full-length aptamer structure, as predicted by secondary structure analyses.[6,12,14] By substituting thymine with cytosine at position 42, we achieved full 9 base-pair hybridization in the internal stem, creating the variant P27.i (Fig. 4A). Subsequently, we extended the lower stem by adding thymine–adenine pairs to create variants P27.1, P27.2, and P27.3.

Using flow-based SPR, we obtained real-time kinetic sensorgrams at various vancomycin concentrations, with washing steps demonstrating reversibility for each split-aptamer pair (ESI Fig. 5†). The sensor response was determined by simultaneous measurement of reference (split-aptamer without vancomycin) and sensing (with increasing vancomycin concentrations) cycles, followed by reference subtraction. The modified split-aptamer P27.i demonstrated significantly enhanced performance, detecting vancomycin at concentrations as low as 200 nM, well below the detection limit of the original P27 design (Fig. 4B).

The dose–response curves for all modified split-aptamer sandwich assays obtained are presented in Fig. 4C. We observed a significant increase in affinity from P27 to P27.i, with the apparent K_d improving from 17 μM to 2.2 μM, respectively. Moreover, this modification led to a substantial improvement in sensitivity, lowering the LOD from 0.75 μM to 0.14 μM. This marked enhancement in both affinity and sensitivity brings our assay well within the clinically relevant concentration range for vancomycin detection. It is important to note that measurements using different SPR platforms yielded different detection limits (portable SPR: 10 μM *vs.* Biacore: 0.75 μM for P27), which can be attributed to their distinct technical capabilities. The Biacore system, offering continuous measurement with higher sensitivity, provides superior detection compared to the steady-state measurements with a lower sensitivity portable SPR system. This instrumental difference explains why qualitative screening was performed using portable SPR for rapid assessment of split-aptamer designs, while precise kinetic measurements were conducted using the Biacore system.

Extended split-aptamer pairs exhibited a range of binding affinities correlating with their base-pair numbers. While P27.1 showed similar K_d and LOD values to the original P27, increasing base-pairs led to significant improvements: P27.2 demonstrated a four-fold decrease in LOD to 0.15 μM with a K_d of 2 μM. P27.3, containing the highest number of base pairs, showed the strongest affinity with K_d less than 1 μM, demonstrating that affinity increases with base pair number. Notably, the K_d of P27.3 approaches that of the full-length aptamer (K_d of 0.25 μM), suggesting that increased base pairing helps restore the binding characteristics of the original aptamer. Correspondingly, the detection limits improved with increased affinity – P27.3 achieved an LOD in the 0.05 μM range, while P27 showed an LOD of 0.8 μM.

However, we noted that more stable stems with higher numbers of complementary base pairs potentially increased the affinity between the two split-aptamer sequences, leading to DNA hybridization in the absence of vancomycin. This resulted in higher background signals and delayed reversibility, particularly evident in the P27.i, which showed an increased response at 0 μM vancomycin compared to the original P27 pair (ESI Fig. 5†). The higher affinity pairs such as P27.2 and P27.3 also demonstrated higher response in the reference cycle (shown in grey). To isolate the specific vancomycin-induced response, this background has been subtracted prior to calculating the dose–response curves presented. A performance matrix summarizing K_d, LOD, and calculated dissociation rates (k_{off}) for all tested modifications is presented in Fig. 4D. Notably, the sensorgrams in ESI Fig. 5† demonstrate complete reversibility for all five aptamer pairs.

As expected, higher affinity pairs exhibit a slower k_{off}, ranging from 18.2 min^{-1} for P27 to 2.7 min^{-1} for the P27.3 pair. These values align well with other reversible biosensors, such as the doxorubicin electrochemical aptamer-based biosensor, which exhibits a k_{off} of 1.35 min^{-1}.[33] Importantly, even the aptamer pairs with enhanced sensitivity maintained relatively fast dissociation rates. This characteristic ensures high temporal resolution, making these assays compatible with real-time continuous monitoring applications. The combination of improved sensitivity and maintained rapid dissociation kinetics in our modified split-aptamer pairs represents a significant advancement.

We also explored different modifications aimed at combining extended complementary stems with enlarged structural loops. One such example, P27.2.o2, was to extend the lower loop by substituting two cytosine (C) from the original P27 to guanine (G) (ESI Fig. 6†). However, secondary structure prediction (mfold[24]) revealed a destabilized aptamer structure due to an extended overhang and a closed lower loop, resulting in a lack of observable binding with the analyte. This outcome,

combined with our CD experiments, confirms that P27 is functional and specific, with minimal non-specific interactions between vancomycin with DNA molecules.[34] Based on our findings and previous truncation studies,[6,12] we hypothesize that the stability of the lower loop region of the complex is indeed crucial for vancomycin interaction. This comprehensive analysis of various modifications provides valuable insights into the structure–function relationship of our split-aptamer system, guiding future optimization strategies for balancing the sensitivity, affinity, and reversibility of split-aptamer assays for the detection of vancomycin and other small molecules.

Vancomycin detection in complex biological matrices

Building upon our comprehensive characterization of the split-aptamer assay performance under varying pH and ionic conditions, we sought to evaluate its functionality in a complex, biologically relevant matrix mimicking the brain tissue of rodents. While our previous experiments in controlled buffer systems demonstrated the robustness of the assay to physiological fluctuations in pH and divalent cation concentrations (Fig. 3, ESI Fig. 3†), biological fluids present additional challenges due to their complex, heterogeneous composition. To bridge the gap between controlled buffers and brain tissue conditions, we first tested the assay in aCSF, which mimics the ionic composition of CSF but lacks proteins and other biomolecules. We then progressed to testing in dog CSF and rat plasma diluted to a comparable level of proteins in the brain interstitial fluid, both containing the full spectrum of biological components. This stepwise approach allowed us to assess how the presence of additional biological factors beyond ions and pH might impact the assay performance and reliability in real-world applications.

To assess the performance of our P27 and the modified P27.i split-aptamer assays in a physiologically relevant complex matrix, we used dog CSF spiked with 20 μM vancomycin. Fig. 5A compares the response in dog CSF to that in aCSF. For the P27 assay, the overall average response signal is roughly half between aCSF and dog CSF, with a fold-change of 0.52. When employing the use of the modified aptamer pair P27.i, the overall average response is about 30% lower between the two matrices (fold-change of 0.72), showing that P27.i, besides presenting higher sensitivity (Fig. 4C), also presents better robustness when in contact with undiluted biological fluids. These results demonstrate that the assay maintains its functionality in relevant biological fluids albeit with a decreased signal output. Additionally, we have also observed slightly lower reproducibility in dog CSF measurements from repetitive measurements in the same sensor (Fig. 5A). Given our extensive characterization of the assay robustness to ionic and pH fluctuations (Fig. 3 and ESI Fig. 3†), we believe these factors are unlikely to be the primary sources of the lower output and increased variability in dog CSF. Instead, we hypothesize that the complex composition of biological CSF, including proteins (the protein profile shown in ESI Fig. 7†), may contribute to this variability. These additional components, absent in our model buffers, could potentially cause fouling of the gold sensor surface, leading to more variable measurements. With improved sensor surface anti-fouling protection, such variations are expected to be significantly reduced.[10,35–37]

To evaluate the long-term stability of our sensor for extended measurements in complex matrices, we employed a CSF surrogate due to the limited availability of real CSF. Based on previous studies utilizing HPLC-MS analysis, we used 200-fold diluted plasma, which has been shown to mimic the complexity of CSF.[38,39] We confirmed this in-house through protein profile comparison using SDS-PAGE (ESI Fig. 7†). Using 200-fold diluted rat plasma in aCSF, we conducted repeated injections of 50 μM vancomycin every 20 min for 2 h, followed by hourly injections for a total of 9 h (Fig. 5B). After each 10 min binding measurement, the sensor surface was washed for 10 min with plasma-spiked aCSF buffer to assess reversibility and robustness.

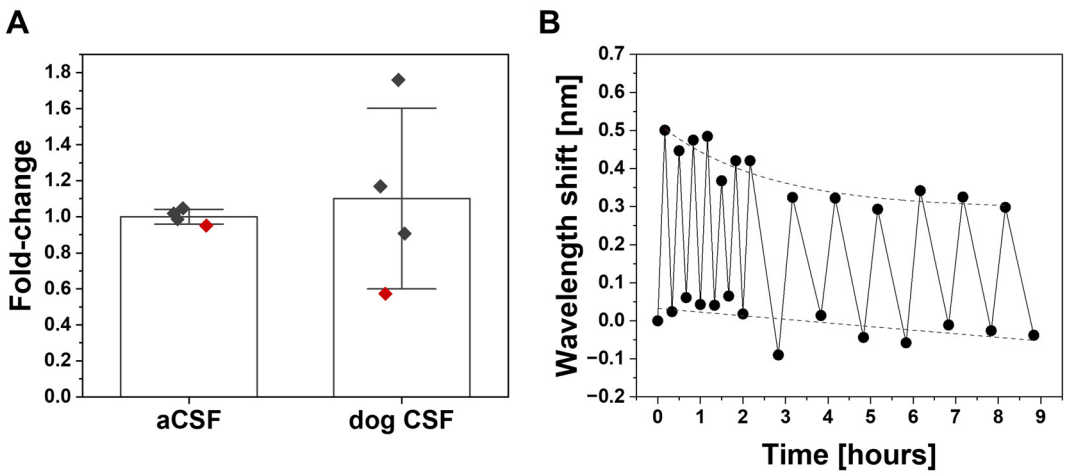

Fig. 5 Split-aptamer assay performance and long-term stability evaluation in complex matrices. (A) Comparison of the sensor response to 20 μM vancomycin in aCSF and dog CSF. Data represent measurements in 2 different sensors (different symbols), normalized to the average value in aCSF. (B) Long-term stability and reproducibility assessment of P27 response to 50 μM vancomycin over 9 h of measurements in plasma diluted in aCSF.

The first two hours (6 short-interval injections) showed ~16% signal loss, while the subsequent 7 h with longer injection intervals resulted in a more significant signal loss of ~48%. Despite this decline, the baseline fitted with a linear regression showed a slope very close to zero (−0.00615), indicating minimal drift. This demonstrates that our assay maintains efficient reversibility even in complex matrices in the presence of proteins during extended sensing experiments. For the scope of the present work, our sensor architecture employs minimal anti-fouling protection, limited to short PEG passivation of the surface prior to aptamer immobilization. The results presented in Fig. 5 demonstrate that while our split-aptamer sensor maintains reversibility in protein-containing environments, signal degradation over time (50% loss after 7 h) indicates the need for additional surface protection strategies for long-term monitoring applications.

This performance provides a promising foundation for future developments. To further enhance the stability and longevity of our sensor for real-time *in vivo* monitoring applications, several strategies could be implemented in future iterations. These include anti-fouling strategies[10,35–37] to minimize non-specific interactions and reduce signal drift over time. This would be especially required for *in vivo* conditions with increasing complexity such as sensing in environments containing higher protein contents like blood or tissue. Additionally, incorporating modifications for enzymatic resistance against naturally occurring DNases[40,41] could significantly improve the stability and lifespan of the aptamer components in biological environments. This work thus lays the groundwork for developing robust, long-lasting biosensors capable of real-time molecular monitoring in complex biological settings.

Conclusions

In this study, we have successfully selected and characterized a split-aptamer sandwich assay for the real-time, label-free monitoring of vancomycin using SPR. Our strategy of splitting an existing aptamer sequence and optimizing its performance for SPR-based detection allows the label-free signal for small molecule detection. Our strategic split-aptamer pair designs yielded significant improvements in sensitivity and yet maintained reversibility, a crucial feature for continuous monitoring applications. Through extensive characterization under various physiological conditions, including pH and ion concentration fluctuations, we have demonstrated the robustness of our assay in environments mimicking those encountered *in vivo*.

Our investigations in complex biological matrices, including dog CSF and diluted rat plasma, show promise for the potential application of this sensor in real-world clinical settings. The ability of the sensor to function in these complex environments, albeit with increased variability, represents a significant step towards *in vivo* monitoring capabilities. The long-term stability studies, demonstrating functionality over nine hours in a plasma-based surrogate, further underscore the potential of this approach for extended real-time monitoring of vancomycin levels.

Looking ahead, several avenues for expansion and improvement of this approach present themselves. The implementation of advanced anti-fouling strategies and modifications for enzymatic resistance could significantly enhance the sensor stability and longevity in biological environments. Incorporation of metal nanoparticles for SPR signal enhancement[42,43] or the use of SPR set-ups with increased sensitivity[44] is known to improve the detection limits and overall sensitivity of the assay, allowing for the monitoring of drugs at lower concentrations. However, for potential *in vivo* applications, a self-containing strategy must be in place to achieve the continuous sensing of a split-aptamer based sensor. The principles developed in this study could be extended to other small molecule targets, potentially broadening the scope of SPR-based or other optical biosensors in therapeutic drug monitoring and pharmacokinetic studies. As we continue to refine and expand our approach, we anticipate the integration of optical biosensors into clinical settings, offering real-time, continuous monitoring of drug levels and potentially revolutionizing personalized medicine approaches in antibiotic treatments and beyond.

Data availability

The data supporting this article have been included as part of the ESI.†

Conflicts of interest

There are no conflicts to declare.

Acknowledgements

We would like to thank Professor Matthias Mayer and Dr Lukas Rohland from Zentrum für Molekulare Biologie der Universität Heidelberg (ZMBH) for their assistance with CD measurements and thank Dr Karine Lapouge and Dr Peter Sehr from EMBL Heidelberg for performing the Biacore experiments. This work was supported by funding from BioMed X Institute to K.S. from Boehringer Ingelheim GmbH.

References

1 A. Meneghello, S. Tartaggia, M. D. Alvau, F. Polo and G. Toffoli, Biosensing Technologies for Therapeutic Drug Monitoring, *Curr. Med. Chem.*, 2018, **25**(34), 4354–4377, DOI: 10.2174/0929867324666170720101736.

2 R. D. Mishi, M. A. Stokes, C. A. Campbell, K. W. Plaxco and S. L. Stocker, Real-Time Monitoring of Antibiotics in the

Critically Ill Using Biosensors, *Antibiotics*, 2023, **12**(10), 1478, DOI: 10.3390/antibiotics12101478.

3 S. Bian, B. Zhu, G. Rong and M. Sawan, Towards Wearable and Implantable Continuous Drug Monitoring: A Review, *J. Pharm. Anal.*, 2021, **11**(1), 1–14, DOI: 10.1016/j.jpha.2020.08.001.

4 N. Haddad, M. Carr, S. Balian, J. Lannin, Y. Kim, C. Toth and J. Jarvis, The Blood–Brain Barrier and Pharmacokinetic/Pharmacodynamic Optimization of Antibiotics for the Treatment of Central Nervous System Infections in Adults, *Antibiotics*, 2022, **11**(12), 1843, DOI: 10.3390/antibiotics11121843.

5 F. Schneider, A. Gessner and N. El-Najjar, Efficacy of Vancomycin and Meropenem in Central Nervous System Infections in Children and Adults: Current Update, *Antibiotics*, 2022, **11**(2), 173, DOI: 10.3390/antibiotics11020173.

6 A. Shaver, J. D. Mahlum, K. Scida, M. L. Johnston, M. Aller Pellitero, Y. Wu, G. V. Carr and N. Arroyo-Currás, Optimization of Vancomycin Aptamer Sequence Length Increases the Sensitivity of Electrochemical, Aptamer-Based Sensors In Vivo, *ACS Sens.*, 2022, **7**(12), 3895–3905, DOI: 10.1021/acssensors.2c01910.

7 M.-C. Fan, J.-L. Sun, J. Sun, J.-W. Ma, N. Wang and W. Fang, The CSF Vancomycin Concentration in Patients With Post-Operative Intracranial Infection Can Be Predicted by the WBCs to Total Cells Ratio and the Serum Trough Concentration, *Front. Neurol.*, 2022, **13**, 893089, DOI: 10.3389/fneur.2022.893089.

8 X. Qi, X. Yan, Y. Zhao, L. Li and S. Wang, Highly Sensitive and Specific Detection of Small Molecules Using Advanced Aptasensors Based on Split Aptamers: A Review, *TrAC, Trends Anal. Chem.*, 2020, **133**, 116069, DOI: 10.1016/j.trac.2020.116069.

9 K. Sergelen, B. Liedberg, W. Knoll and J. Dostálek, A Surface Plasmon Field-Enhanced Fluorescence Reversible Split Aptamer Biosensor, *Analyst*, 2017, **142**(16), 2995–3001, DOI: 10.1039/C7AN00970D.

10 Y. Taguchi, K. Toma, K. Iitani, T. Arakawa, Y. Iwasaki and K. Mitsubayashi, In Vitro Performance of a Long-Range Surface Plasmon Hydrogel Aptasensor for Continuous and Real-Time Vancomycin Measurement in Human Serum, *ACS Appl. Mater. Interfaces*, 2024, **16**(22), 28162–28171, DOI: 10.1021/acsami.4c03805.

11 N. Arroyo-Currás, J. Somerson, P. A. Vieira, K. L. Ploense, T. E. Kippin and K. W. Plaxco, Real-Time Measurement of Small Molecules Directly in Awake, Ambulatory Animals, *Proc. Natl. Acad. Sci. U. S. A.*, 2017, **114**(4), 645–650, DOI: 10.1073/pnas.1613458114.

12 P. Dauphin-Ducharme, K. Yang, N. Arroyo-Currás, K. L. Ploense, Y. Zhang, J. Gerson, M. Kurnik, T. E. Kippin, M. N. Stojanovic and K. W. Plaxco, Electrochemical Aptamer-Based Sensors for Improved Therapeutic Drug Monitoring and High-Precision, Feedback-Controlled Drug Delivery, *ACS Sens.*, 2019, **4**(10), 2832–2837, DOI: 10.1021/acssensors.9b01616.

13 A. Stuber and N. Nakatsuka, Aptamer Renaissance for Neurochemical Biosensing, *ACS Nano*, 2024, **18**(4), 2552–2563, DOI: 10.1021/acsnano.3c09576.

14 M.-D. Nguyen, M. T. Osborne, G. T. Prevot, Z. R. Churcher, P. E. Johnson, L. Simine and P. Dauphin-Ducharme, Truncations and *in Silico* Docking to Enhance the Analytical Response of Aptamer-Based Biosensors, *Biosens. Bioelectron.*, 2024, **265**, 116680, DOI: 10.1016/j.bios.2024.116680.

15 A. M. Onaș, C. Dascălu, M. D. Raicopol and L. Pilan, Critical Design Factors for Electrochemical Aptasensors Based on Target-Induced Conformational Changes: The Case of Small-Molecule Targets, *Biosensors*, 2022, **12**(10), 816, DOI: 10.3390/bios12100816.

16 N. Nakatsuka, Aptamer-Field-Effect Transistors for Small-Molecule Sensing in Complex Environments, in *Nucleic Acid Aptamers: Selection, Characterization, and Application*, ed. G. Mayer and M. M. Menger, Springer US, New York, NY, 2023, pp. 187–196. DOI: 10.1007/978-1-0716-2695-5_14.

17 B. Wang, C. Zhao, Z. Wang, K.-A. Yang, X. Cheng, W. Liu, W. Yu, S. Lin, Y. Zhao, K. M. Cheung, H. Lin, H. Hojaiji, P. S. Weiss, M. N. Stojanović, A. J. Tomiyama, A. M. Andrews and S. Emaminejad, Wearable Aptamer-Field-Effect Transistor Sensing System for Noninvasive Cortisol Monitoring, *Sci. Adv.*, 2022, **8**(1), eabk0967, DOI: 10.1126/sciadv.abk0967.

18 G. Wu, N. Zhang, A. Matarasso, I. Heck, H. Li, W. Lu, J. G. Phaup, M. J. Schneider, Y. Wu, Z. Weng, H. Sun, Z. Gao, X. Zhang, S. G. Sandberg, D. Parvin, E. Seaholm, S. K. Islam, X. Wang, P. E. M. Phillips, D. C. Castro, S. Ding, D.-P. Li, M. R. Bruchas and Y. Zhang, Implantable Aptamer-Graphene Microtransistors for Real-Time Monitoring of Neurochemical Release in Vivo, *Nano Lett.*, 2022, **22**(9), 3668–3677, DOI: 10.1021/acs.nanolett.2c00289.

19 K. Sergelen, S. Fossati, A. Turupcu, C. Oostenbrink, B. Liedberg, W. Knoll and J. Dostálek, Plasmon Field-Enhanced Fluorescence Energy Transfer for Hairpin Aptamer Assay Readout Sup Info, *ACS Sens.*, 2017, **2**(7), 916–923, DOI: 10.1021/acssensors.7b00131.

20 F. Melaine, Y. Roupioz and A. Buhot, Gold Nanoparticles Surface Plasmon Resonance Enhanced Signal for the Detection of Small Molecules on Split-Aptamer Microarrays (Small Molecules Detection from Split-Aptamers), *Microarrays*, 2015, **4**(1), 41–52, DOI: 10.3390/microarrays4010041.

21 Y. Tang, F. Long, C. Gu, C. Wang, S. Han and M. He, Reusable Split-Aptamer-Based Biosensor for Rapid Detection of Cocaine in Serum by Using an All-Fiber Evanescent Wave Optical Biosensing Platform, *Anal. Chim. Acta*, 2016, **933**, 182–188, DOI: 10.1016/j.aca.2016.05.021.

22 N. Nakatsuka, J. M. Abendroth, K. A. Yang and A. M. Andrews, Divalent Cation Dependence Enhances Dopamine Aptamer Biosensing, *ACS Appl. Mater. Interfaces*, 2021, **13**(8), 9425–9435, DOI: 10.1021/acsami.0c17535.

23 Q. Wang, J. Huang, X. Yang, K. Wang, L. He, X. Li and C. Xue, Surface Plasmon Resonance Detection of Small

Molecule Using Split Aptamer Fragments, *Sens. Actuators, B*, 2011, **156**(2), 893–898, DOI: 10.1016/j.snb.2011.03.002.

24 M. Zuker, Mfold Web Server for Nucleic Acid Folding and Hybridization Prediction, *Nucleic Acids Res.*, 2003, **31**(13), 3406–3415, DOI: 10.1093/nar/gkg595.

25 *Magnesium in the Central Nervous System*, ed. R. Vink and M. Nechifor, Series, University of Adelaide Press, 2011.

26 E. M. Kawamoto, C. Vivar and S. Camandola, Physiology and Pathology of Calcium Signaling in the Brain, *Front. Pharmacol.*, 2012, **3**(61), 1–17, DOI: 10.3389/fphar.2012.00061.

27 E. Ruusuvuori and K. Kaila, Carbonic Anhydrases and Brain PH in the Control of Neuronal Excitability, in *Carbonic anhydrase: mechanism, regulation, links to disease, and industrial applications*, 2014, pp. 271–290.

28 R. Mitchell and M. Singer, Respiration and Cerebrospinal Fluid PH in Metabolic Acidosis and Alkalosis, *J. Appl. Physiol.*, 1965, **20**(5), 905–911.

29 K. Steiner and C. Humpel, Effects of Ischemia on the Migratory Capacity of Microglia Along Collagen Microcontact Prints on Organotypic Mouse Cortex Brain Slices, *Front. Cell. Neurosci.*, 2022, **16**, 858802, DOI: 10.3389/fncel.2022.858802.

30 M. Forsberg, H. Seth, A. Björefeldt, T. Lyckenvik, M. Andersson, P. Wasling, H. Zetterberg and E. Hanse, Ionized Calcium in Human Cerebrospinal Fluid and Its Influence on Intrinsic and Synaptic Excitability of Hippocampal Pyramidal Neurons in the Rat, *J. Neurochem.*, 2019, **149**(4), 452–470, DOI: 10.1111/jnc.14693.

31 M. J. Rybak, J. Le, T. P. Lodise, D. P. Levine, J. S. Bradley, C. Liu, B. A. Mueller, M. P. Pai, A. Wong-Beringer, J. C. Rotschafer, K. A. Rodvold, H. D. Maples and B. M. Lomaestro, Therapeutic Monitoring of Vancomycin for Serious Methicillin-Resistant Staphylococcus Aureus Infections: A Revised Consensus Guideline and Review by the American Society of Health-System Pharmacists, the Infectious Diseases Society of America, the Pediatric Infectious Diseases Society, and the Society of Infectious Diseases Pharmacists, *Am. J. Health-Syst. Pharm.*, 2020, **77**(11), 835–864, DOI: 10.1093/ajhp/zxaa036.

32 J. Gerson, M. K. Erdal, P. Dauphin-Ducharme, A. Idili, J. P. Hespanha, K. W. Plaxco and T. E. Kippin, A High-Precision View of Intercompartmental Drug Transport via Simultaneous, Seconds-Resolved, in Situ Measurements in the Vein and Brain, *Br. J. Pharmacol.*, 2024, **181**(20), 3869–3885, DOI: 10.1111/bph.16471.

33 B. S. Ferguson, D. A. Hoggarth, D. Maliniak, K. Ploense, R. J. White, N. Woodward, K. Hsieh, A. J. Bonham, M. Eisenstein, T. E. Kippin, K. W. Plaxco and H. T. Soh, Real-Time, Aptamer-Based Tracking of Circulating Therapeutic Agents in Living Animals, *Sci. Transl. Med.*, 2013, **5**(213), 213ra165, DOI: 10.1126/scitranslmed.3007095.

34 L. Kong, Z. Liu, S. Liu and D. Wang, Interaction of Vancomycin with DNA, and Determination of DNA via Resonance Rayleigh Scattering and Resonance Nonlinear Scattering, *Anal. Methods*, 2012, **4**(12), 4346–4352, DOI: 10.1039/C2AY26050F.

35 R. D'Agata, N. Bellassai, V. Jungbluth and G. Spoto, Recent Advances in Antifouling Materials for Surface Plasmon Resonance Biosensing in Clinical Diagnostics and Food Safety, *Polymers*, 2021, **13**(12), 1929, DOI: 10.3390/polym13121929.

36 Z. Song, R. Han, K. Yu, R. Li and X. Luo, Antifouling Strategies for Electrochemical Sensing in Complex Biological Media, *Microchim. Acta*, 2024, **191**(3), 138, DOI: 10.1007/s00604-024-06218-2.

37 M. Soler and L. M. Lechuga, Biochemistry Strategies for Label-Free Optical Sensor Biofunctionalization: Advances towards Real Applicability, *Anal. Bioanal. Chem.*, 2022, **414**(18), 5071–5085, DOI: 10.1007/s00216-021-03751-4.

38 S. Hooshfar, B. Basiri and M. G. Bartlett, Development of a Surrogate Matrix for Cerebral Spinal Fluid for Liquid Chromatography/Mass Spectrometry Based Analytical Methods, *Rapid Commun. Mass Spectrom.*, 2016, **30**(7), 854–858, DOI: 10.1002/rcm.7509.

39 J. R. Fogh, A.-M. Jacobsen, T. T. T. N. Nguyen, K. D. Rand and L. R. Olsen, Investigating Surrogate Cerebrospinal Fluid Matrix Compositions for Use in Quantitative LC-MS Analysis of Therapeutic Antibodies in the Cerebrospinal Fluid, *Anal. Bioanal. Chem.*, 2020, **412**(7), 1653–1661, DOI: 10.1007/s00216-020-02403-3.

40 K. K. Leung, J. Gerson, N. Emmons, J. M. Heemstra, T. E. Kippin and K. W. Plaxco, The Use of Xenonucleic Acids Significantly Reduces TheIn Vivo Drift of Electrochemical Aptamer-Based Sensors, *Angew. Chem., Int. Ed.*, 2024, **63**, e202316678, DOI: 10.1002/anie.202316678.

41 Y. Zhao, A. Sarkar and X. Wang, Peptide Nucleic Acid Based Tension Sensor for Cellular Force Imaging with Strong DNase Resistance, *Biosens. Bioelectron.*, 2020, **150**, 111959, DOI: 10.1016/j.bios.2019.111959.

42 A. Kausaite-Minkstimiene, A. Popov and A. Ramanaviciene, Surface Plasmon Resonance Immunosensor with Antibody-Functionalized Magnetoplasmonic Nanoparticles for Ultrasensitive Quantification of the CD5 Biomarker, *ACS Appl. Mater. Interfaces*, 2022, **14**(18), 20720–20728, DOI: 10.1021/acsami.2c02936.

43 G. E. Yılmaz, Y. Saylan, I. Göktürk, F. Yılmaz and A. Denizli, Selective Amplification of Plasmonic Sensor Signal for Cortisol Detection Using Gold Nanoparticles, *Biosensors*, 2022, **12**(7), 482, DOI: 10.3390/bios12070482.

44 M. Qi, N. M. Y. Zhang, K. Li, S. C. Tjin and L. Wei, Hybrid Plasmonic Fiber-Optic Sensors, *Sensors*, 2020, **20**(11), 3266, DOI: 10.3390/s20113266.